Brain, Behavior, and Immunity 115 (2024) 718–726

Contents lists available at ScienceDirect

Brain Behavior and Immunity

journal homepage: www.elsevier.com/locate/ybrbi

Short Communication

Stem-cell derived neurosphere assay highlights the effects of viral infection on human cortical development

Edward Drydale [a,2], Phalguni Rath [a,2], Katie Holden [a,2], Gregory Holt [a], Laurissa Havins [a,b], Thomas Johnson [a], James Bancroft [a,1], Lahiru Handunnetthi [a,b,1,*]

[a] Wellcome Centre for Human Genetics, University of Oxford, Roosevelt Drive, OX3 9DU, United Kingdom
[b] Nuffield Department of Clinical Neurosciences, Level 6, West Wing, John Radcliffe Hospital, University of Oxford, OX3 9DU, United Kingdom

ARTICLE INFO

Keywords:
Neurodevelopmental disorders
Stem cells
Infection
Cortex

ABSTRACT

Aberrant cortical development is a key feature of neurodevelopmental disorders such as autism spectrum disorder and schizophrenia. Both genetic and environmental risk factors are thought to contribute to defects in cortical development; however, model systems that can capture the dynamic process of human cortical development are not well established. To address this challenge, we combined recent progress in induced pluripotent stem cell differentiation with advanced live cell imaging techniques to establish a novel three-dimensional neurosphere assay, amenable to genetic and environmental modifications, to investigate key aspects of human cortical development in real-time. For the first time, we demonstrate the ability to visualise and quantify radial glial extension and neural migration through live cell imaging. To show proof-of-concept, we used our neurosphere assay to study the effect of a simulated viral infection, a well-established environmental risk factor in neurodevelopmental disorders, on cortical development. This was achieved by exposing neurospheres to the viral mimic, polyinosinic:polycytidylic acid. The results showed significant reductions in radial glia growth and neural migration in three independent differentiations. Further, fixed imaging highlighted reductions in the *HOPX*-expressing outer radial glia scaffolding and a consequent decrease in the migration of *CTIP2*-expressing cortical cells. Overall, our results provide new insight into how infections may exert deleterious effects on the developing human cortex.

1. Introduction

The cerebral cortex is responsible for higher cognitive function in humans. It is a laminated structure that contains a bewildering diversity of neurons and complex networks of connections. Intriguingly, these cortical cells can be traced back to just a few neuronal progenitors at the start of cortical neurogenesis (Miller et al., 2019). Through a set of tightly coordinated events, these neuronal progenitors undergo proliferation, migration, differentiation, and functional integration into neuronal circuitry (Miller et al., 2019). Defects in this process are thought to contribute to neurodevelopmental disorders such as autism spectrum disorder (ASD) and schizophrenia, affecting more than 1 % of the population worldwide (Frances et al., 2022; Zeidan et al., 2022; Charlson et al., 2018). This is supported by findings that genetic and environmental risk factors in ASD and schizophrenia exert deleterious effects on cortical developmental processes (Gulsuner et al., 2013; Satterstrom et al., 2020; Warre-Cornish et al., 2020; Handunnetthi et al., 2021). An environmental risk factor of interest in neurodevelopmental disorders is viral infection during gestation, which coincides with key cortical developmental processes (Saatci et al., 2021; Jiang et al., 2016). This has been studied in animal models using polyinosinic:polycytidylic acid (polyI:C), a double-stranded synthetic RNA molecule that mimics viral infections (Vasistha et al., 2020; Haddad et al., 2020).

Human cortical development is astonishingly complex (Miller et al., 2019). At the start, neuroepithelial cells transform into radial glia cells, establishing the ventricular zone. The ventricular radial glia cells not only undergo self-renewal but also produce nascent neurons. These neurons then migrate along the radial fibres of ventricular glia to create the deep layers of the cortex. In parallel, the ventricular radial glia cells generate intermediate progenitor cells and outer radial glial cells that

* Corresponding author.
E-mail address: lahiru@well.ox.ac.uk (L. Handunnetthi).
[1] Co-Senior Author.
[2] These authors contributed equally.

https://doi.org/10.1016/j.bbi.2023.11.017
Received 17 March 2023; Received in revised form 5 November 2023; Accepted 16 November 2023
Available online 22 November 2023

migrate into the expanded outer subventricular zone in humans. The outer radial glia cells subsequently develop into the predominant source of neurons that create the upper layers of the cortex and become an essential part of cortical development (Hansen et al., 2010). These finely orchestrated events are susceptible to disruption by genetic and environmental factors linked to neurodevelopmental disorders.

Therefore, modelling aspects of cortical development is a key research goal in neurodevelopmental disorders. However, this has been difficult to achieve for several reasons. First, previous studies have focused on rodent models (Ducker et al., 2020) but human cortical development differs from that of rodents. For example, the outer radial glia population is largely missing in mouse brains, but these cells form an essential part of human cortical development (Hansen et al., 2010). Second, neural cell migration is a highly dynamic process making it difficult to visualise over time. As a result, previous studies have analysed only a few time points in fixed samples, providing poor temporal resolution (Brennand et al., 2015; Delaloy et al., 2010). This lack of temporal resolution has hindered our ability to understand the precise cellular substrates that contribute to neurodevelopmental disorders. To address this challenge, first we combined recent progress in induced pluripotent stem cell (iPSC) differentiation with advanced live cell imaging techniques to establish a novel three-dimensional neurosphere assay, amenable to genetic and environmental modifications. Second, we created an automated pipeline for high throughput image analysis. Subsequently, we applied polyI:C to our neurosphere assay to assess how a simulated viral infection could influence cortical developmental processes.

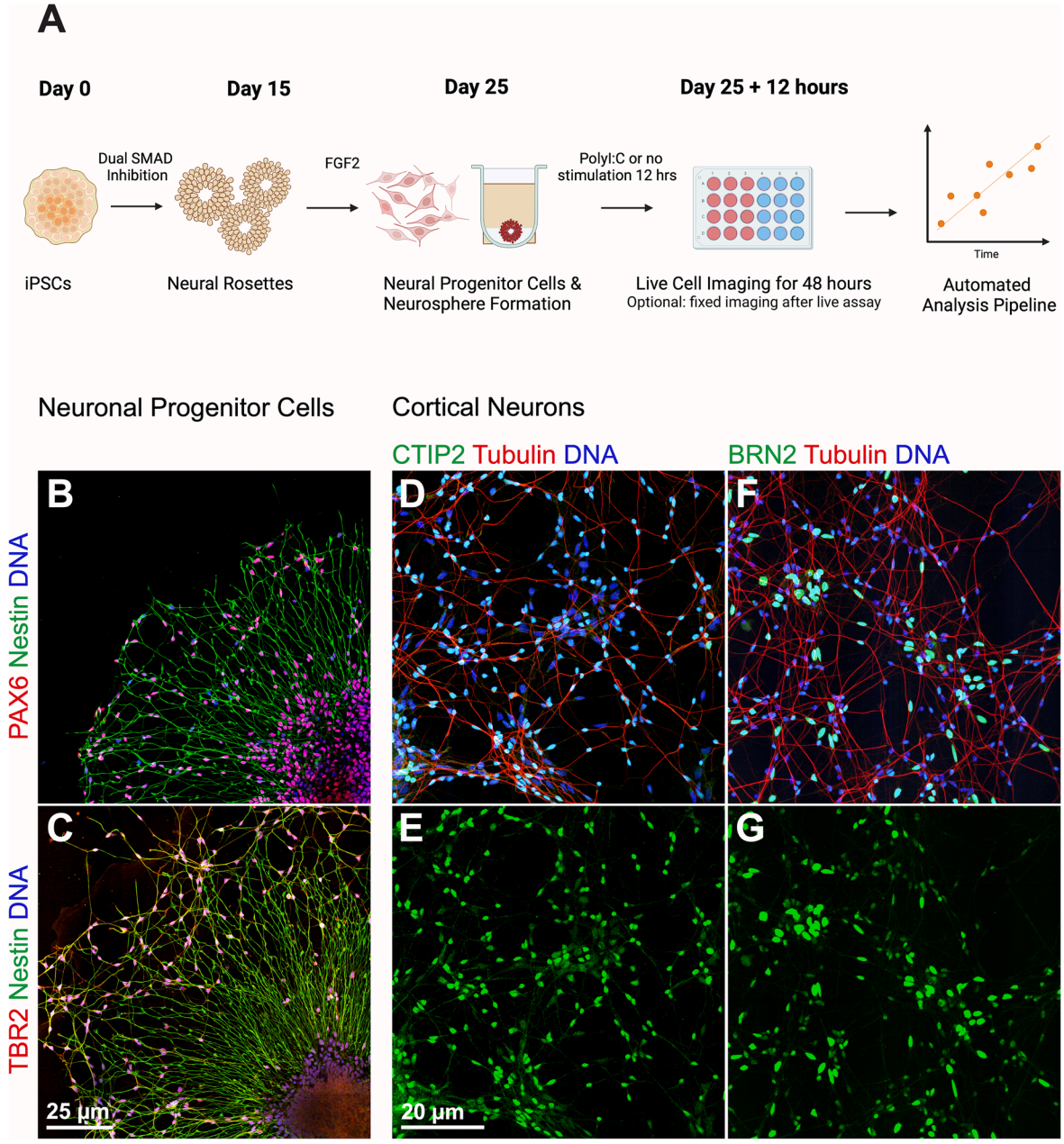

Fig. 1. Experimental pipeline and iPSC derived cortical linage neuronal progenitor cells and cortical neurons. A: Schematic representation of neurosphere formation and live imaging B: PAX6 expressing primary neuronal progenitors. C: TBR2 expressing intermediate neuronal progenitor cells. D and E: CTIP2 expressing deep cortical layer neurons. F and G: BRN2 expressing upper-layer cortical neurons.

2. Materials and methods

2.1. IPSC differentiation and neurosphere formation

HPSI0114i-Kolf_2 human induced pluripotent stem cells from a single donor were purchased from the Wellcome Sanger Institute (Biosample: SAMEA2547615) and maintained in Essential 8 medium (Thermo Fisher Scientific A1517001) on Vitronectin (Thermo Fisher Scientific CTS279S3) coated tissue culture dishes. The iPSC line was karyotypically normal (*supplementary* Fig. 3), their pluripotency was confirmed based on the expression of OCT4 and NANOG using immunofluorescence and flow cytometry (supplementary Figs. 1 and 2). Subsequently, the iPSCs were differentiated into neuronal progenitor cells and cortical neurons as described previously (Shi et al., 2012). Briefly, neuronal induction was carried out using 1uM Dorsomorphin (Bio-Techne, 3093/10) and 10 uM SB431542 (Tocris Bioscience, 1614) in neuronal maintenance medium (NMM) (supplementary table 1). The appearance of a neuroepithelial sheet was noted after 8–12 days. At this point, the neuroepithelial cells were dissociated using 2 mg/mL Dispase II (Gibco™ 17105041) and replated on growth factor reduced matrigel coated plates. Upon appearance of neural rosettes, the cells were maintained in 20 ng/mL FGF2-supplemented NMM for 4 to 5 days.

The experimental pipeline for neurosphere formation to live imaging is schematically summarised in Fig. 1A. On day 25, the cells were dissociated into single cells using Accutase (Gibco™ A1110501) and subsequently reaggregated in 96-well V-bottom plates to form three dimensional neurospheres. Each neurosphere contained approximately 10,000 neuronal progenitors. The experimental condition underwent polyI:C (100 μg/ml) stimulation 12 h prior to the start of live cell imaging. Live imaging of neurospheres took place immediately after the stimulation period on 24 well plates coated with Poly-l-ornithine (Sigma P4957) and Matrigel (Corning, 354230). Three neuronal inductions and differentiations were carried out. These were treated separately throughout neurosphere formation, live imaging and analysis. All neurospheres were constructed at day 25 of the neuronal differentiation to keep developmental timepoint consistent between replicates. A total of 46 neurospheres (corresponding to differentiation 1 = 15 neurospheres, differentiation 2 = 14 neurospheres, and differentiation 3 = 14 neurospheres) were imaged.

The cortical identity of neurospheres was checked based on the appearance of PAX6 expressing primary neuronal progenitors and TBR2 expressing intermediate neuronal progenitors. In parallel, a proportion of neuronal progenitors were further differentiated in 2D culture to confirm the appearance of cortical neurons. After 90 days in culture, the presence of both CTIP2 expressing deep layer and BRN2 expressing upper layer neurons was checked using immunofluorescence.

2.2. Live image acquisition and analysis pipeline

For live cell imaging, neurospheres grown in 24-well optical bottomed plates (Ibidi 82426) were incubated with SiR-Tubulin and SPY-555-DNA at 100 nM concentration 2 h prior to imaging. All images were acquired using an Olympus IXplore Spin-SR, using a 50 μm pinhole confocal spinning disk and a Hamamatsu ORCA Fusion BT camera. 140 μm z-stacks with a z spacing of 10 μm were taken every 30 min over a total time course of 48 h. These stacks were captured as tiled regions using a 10x, 0.4NA air Objective lens. See supplementary table 3 for individual channel and filter details. Live cell migration analysis was performed using an automated pipeline created in Arivis AG, Germany (https://www.arivis.com). First, maximum projections were generated from the image z-stacks. The projected (max-intensity) images were then processed to smooth the channels using closing and mean filters. An intensity threshold was then applied to define the migrating progenitor cells using nuclear staining and radial fibre regions based on tubulin staining. Further filtering to segments was applied based on size to exclude small artifacts, after which the area was calculated at each timepoint.

2.3. Immunofluorescence

Cells grown on 24 well plates (Ibidi 82426) were fixed in 4 % paraformaldehyde for 15 min. The cells were permeabilized using 0.1 % Triton-X100 in PBS for 15 min and blocked for 1 h with 0.5 % BSA in PBS. Subsequently, the cells were stained with primary antibodies diluted in 0.5 % BSA in PBS at 4 °C overnight. Details of primary antibodies can be found in supplementary table 5. The cells were washed and incubated with secondary antibodies (Goat anti-Mouse IgG Alexa Fluor™ 488, Invitrogen A11029, Goat anti-Rabbit IgG, Alexa Fluor™ 568, Invitrogen A11036) diluted 1:1000 in PBS, for 1 h at room temperature. Also, the cells were stained with 1 μM DAPI. Images were acquired using an Olympus IXplore Spin-SR, using a 50 μm pinhole confocal spinning disk and a Hamamatsu ORCA Fusion BT camera. 50 μm z-stacks with a z spacing of 2 μm were captured as tiled regions using a 20x, 0.8NA air objective lens. See supplementary table 4 for individual channel and filter details. Maximum intensity z projections were generated from acquired z stacks and analysed with an automated pipeline created in Arivis. A combination of image pre-processing and segmentation was used to generate regions of interest from which data was generated, details can be found in Supplementary figures 5–7.

2.4. RNA extraction

Neuronal progenitors were plated on 12 well plates (Greiner 665180) and expanded until day 25. At this point, cells underwent polyI:C stimulation or no stimulation. Subsequently, the cells were lysed in RLT buffer (RNeasy mini kit, QIAGEN, 74104). RNA was extracted from lysates using the QIAGEN RNeasy mini kit according to manufacturer's instructions, and included a DNase I treatment step (QIAGEN, 79254). RNA concentrations were measured on a NanoDrop (NanoDrop 1000, Thermo Fisher).

2.5. Quantitative PCR

cDNA was synthesised from 200 ng of total RNA using UltraScript™ cDNA Synthesis Kit (PCR Biosystems, PB30.11–10) in 20 μl total reaction volume. Samples were incubated at 42 °C for 30 min, followed by 10 min at 85 °C to denature RTase. Samples were diluted 1:4 in DNase and RNase free water before use. Quantitative PCR was performed using PowerUp™ SYBR™ Green Master Mix (Thermo Fisher, A25742), set up in 10 μl reactions as per manufacturer's instructions, using 2.5 ng cDNA template. qPCR reactions were performed on the CFX96 Touch Real-Time PCR Detection System (BioRad). Cycling conditions can be found in supplementary table 6. Three biological replicates were tested per condition, and each sample was run in triplicates. Primers (Thermo Fisher) were designed for the housekeeping gene (TBP) and cortical marker gene (CTIP2) using NCBI Primer-BLAST. Sequences can be found in supplementary table 7. PCR results were analysed and the relative gene expression was determined using the ΔΔCT method, using TBP as the reference gene and the average ΔCT values of the WT group as the control.

2.6. Statistical analysis

The '*lmer4*' package in R was used to assess the relationship between time and two separate outcomes of interest in this study, 1) radial glia growth and 2) neural migration. The neurospheres were either unstimulated or stimulated with polyI:C. The following two linear mixed effects models were used to explore the association between time and individual outcomes:

Model 1: Outcome ~ Time + Stimulation Status (1 + Time| Neurospheres).

Model 2: Outcome ~ Time × Stimulation Status (1 + Time|

Neurospheres).

The first model included one fixed effects parameter, status of stimulation with PolyI:C. This modelled two regression lines (stimulated vs. unstimulated) that have different starting points (i.e. intercepts) but the same rate of change in outcome (i.e. identical slopes). The second model included another fixed effects parameter, an interaction term between status of stimulation and time. This modelled two regression lines (stimulated vs. unstimulated) that have different starting points (i.e., intercepts) and different rates of change in outcome (i.e. different slopes). Both models included the following random effects parameters: 1) each neurosphere sample (i.e. random intercepts) and 2) average change in outcome per unit time for each neurosphere sample (i.e. random slopes). A likelihood ratio test was carried out to identify the model with a better fit to the data. In parallel, radial glia growth and neural migration areas in fixed neurosphere were compared between stimulated and unstimulated conditions using a two-tailed *t*-test and a significance threshold of 0.05.

3. Results

3.1. Establishment of IPSC derived neuronal progenitors of cortical lineage

We differentiated human iPSCs into neuronal progenitors and cortical neurons. The cortical linage of these cells was confirmed using immunofluorescence. First, we demonstrated that our iPSC lines retained pluripotency through the expression of *OCT4* and *NANOG* (supplementary Figs. 1 and 2). Second, we confirmed the appearance of primary and intermediate neuronal progenitor cells of cortical linage using *PAX6* and *TBR2* respectively (Fig. 1B and 1C). Third, we demonstrated that these neuronal progenitor cells gave rise to both *CTIP2*-expressing deep cortical neurons and *BRN2*-expressing upper-layer cortical neurons (Fig. 1D-1G).

We used neuronal progenitor cells from day twenty-five of differentiation to make neurospheres (Fig. 1A). We demonstrated the temporal evolution of neurospheres and the appearance of intermediate progenitor cells and cortical neurons using immunofluorescence (Fig. 2A and 2B). Specifically, we found an increasing number of *TBR2* expressing intermediate progenitor cells appearing over time (Fig. 2B). Similarly, an increasing number of nascent *CTIP2* expressing cortical neurons migrated along the radial fibres over time (Fig. 2A).

3.2. Live cell imaging captured and quantified key aspects of human cortical development

We were able visualise key aspects of human cortical development in live cells for the first time. We captured time-lapse images of neurospheres every 30 min over a period of 48 h using Spin-SR microscope system (Olympus) (*video 1*). We captured the growth of radial fibres away from the central mass of cells (Fig. 3A, *bottom panel*) and migration of neural cells along the radial fibres (Fig. 3A, *middle panel*).

We demonstrated the ability to robustly quantify radial glia growth and neural cell migration over time in our live neurosphere assay. The automated pipeline for image analysis successfully defined migrating neural cells and radial fibre extensions based on nuclear and tubulin staining, respectively (*supplementary* Fig. 4 and *supplementary movies 2*

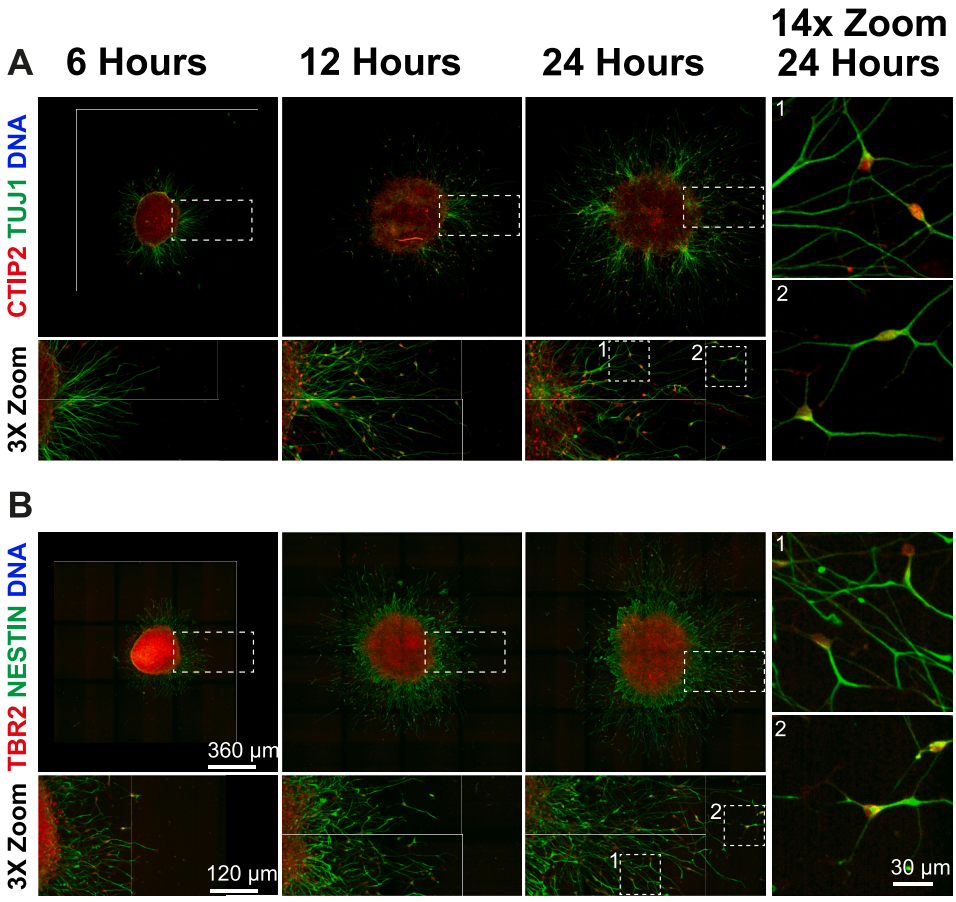

Fig. 2. Evolution of neurospheres over three time points 6-, 12-, and 24-hours using immunofluorescence. Top panel: Appearance of CTIP2 expressing deep cortical layer neurons over time. 3X and 14X zoom panels show the migration and differentiation of CTIP2 expressing neurons as they reach the outer edge of neurospheres. Bottom panel: Appearance of TBR2 expressing intermediate neuronal progenitor cells over time. 3X and 14X zoom panels show the appearance of TBR2 expressing intermediate neuronal progenitors within the radial extensions of neurospheres over time.

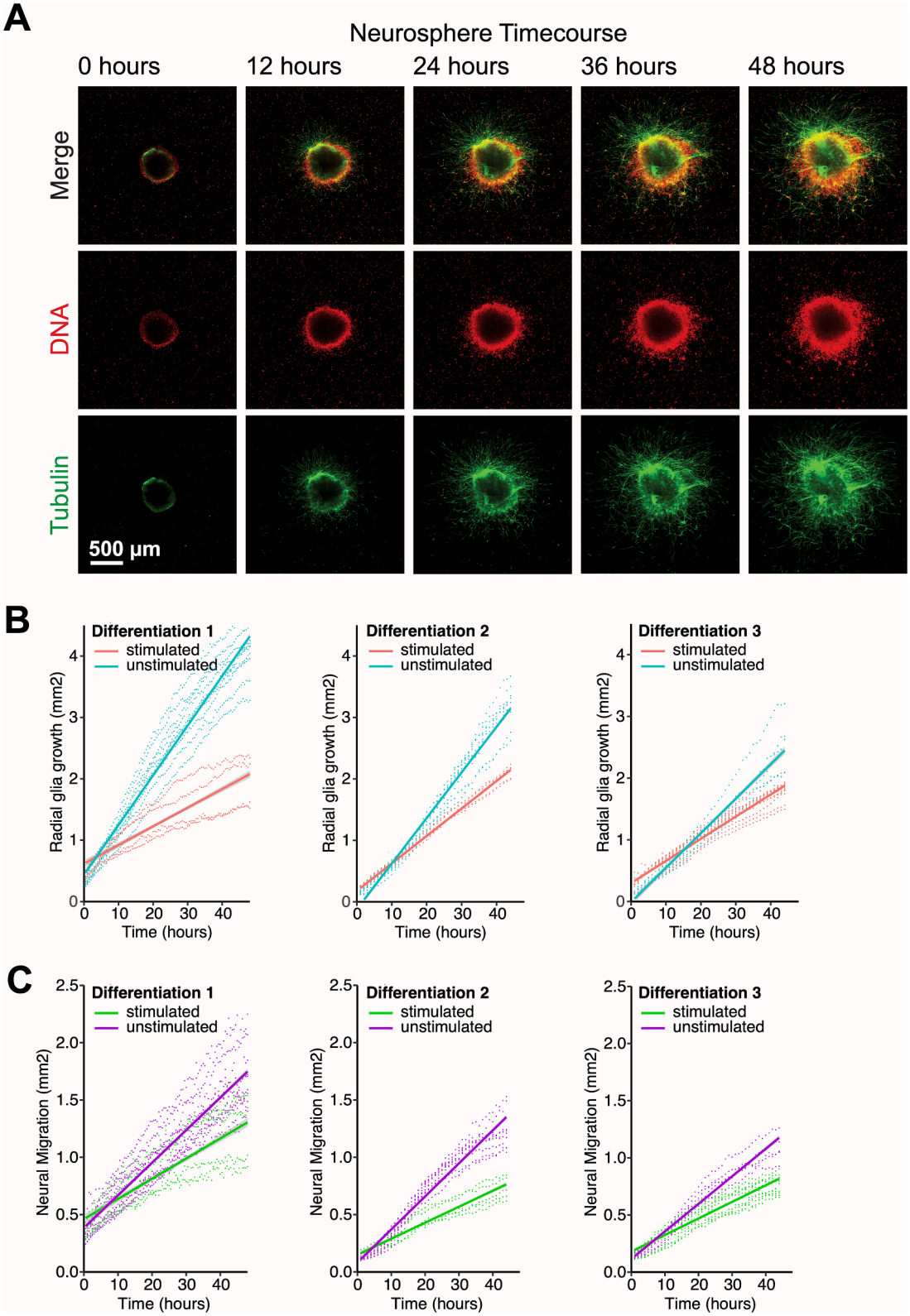

Fig. 3. Evolution of neurospheres over time using live cell imaging and their quantification. A: Single neurosphere over time as observed through live imaging at four selected time points. The top panel shows combined radial glia (Tubulin) and nuclei of migrating neural cells (DNA) at four selected time points 0, 12, 24, 36 and 48 h. The middle and bottom panels show the breakdown of nuclei of migrating neural cells (DNA) and radial glia (Tubulin) respectively at 0, 12, 24, 36 and 48 h. The middle and bottom panels show the breakdown of nuclei of migrating neural cells and radial glia respectively at time points 0, 12, 24, 36 and 48 h. B: Radial glia growth over time in each individual neurosphere is presented for three separate neuronal differentiations. Colours represent the stimulation status, red = polyI:C stimulation and blue = no stimulation. The solid line is the mixed effects linear models showing radial glia extension based on stimulation status over time. The grey area is the 95 % confidence interval. C: Neural migration over time in each individual neurosphere is presented for three separate neuronal differentiations. Colours represent the stimulation status, green = polyI:C stimulation and purple = no stimulation. The solid line is the mixed effects linear models showing radial glia extension based on stimulation status over time. The grey area is the 95 % confidence interval.

and 3). Quantification of radial glia growth and neural migration for individual neurospheres was carried out for three separate neuronal differentiations and subsequent neurosphere assays as shown in Fig. 3B and 3C, respectively.

3.3. Viral mimic polyI:C disrupts neural migration and radial fibre extension over time

We used polyI:C, a well-established viral mimic through its effects specifically on the Toll-like receptor 3 pathway, to recapitulate infection twelve hours prior to live imaging. Linear mixed effects model showed that radial glia growth was greater in unstimulated neurospheres relative to stimulated neurospheres by 0.028 mm^2/hour (SE:0.0046 mm^2/hour, p = 1.78e-05) for Differentiation 1, 0.029 mm^2/hour (SE:0.0040 mm^2/hour, p = 3.6e-06) for Differentiation 2, and 0.020 mm^2/hour (SE:0.0030 mm^2/hour, p = 4.27e-06) (Fig. 3B). A likelihood-ratio test indicated that a model that included the interaction between time and stimulation status (i.e. allowing different rates of growth based on stimulation status) was better fit for radial glial growth data ($\chi2 = 18.9$p = 1.33e-05 for Differentiation 1, $\chi2 = 22.2$p = 2.55e-06 for Differentiation 2, $\chi2 = 21.7$p = 3.18e-06 for Differentiation 3). Also, linear mixed effects model identified that neural cell migration was greater in unstimulated neurospheres by 0.011 mm^2/hour (SE:0.0025 mm^2/hour, P = 0.0009) for Differentiation 1, 0.015 mm^2/hour (SE:0.0018 mm^2/hour, P = 1.56e-06) for Differentiation 2 and 0.010 mm^2/hour (SE:0.001 mm^2/hour, P = 3.21e-08) (Fig. 3C). Similarly, a model that included the interaction between time and stimulation status (i.e. allowing different rates of growth based on stimulation status) was a better fit for neural migration data ($\chi2 = 11.5$, p = 0.0007 for Differentiation 1, $\chi2 = 23.9$, p = 1.07e-06 for Differentiation 2, $\chi2 = 31.4$, p = 2.11e-08 for Differentiation 3).

To further understand the effects of polyI:C on cortical development, we carried out a series of immunofluorescence experiments using fixed neurospheres after 48 h of growth (Fig. 4). In line with our results from the live cell assay, we found that polyI:C stimulation resulted in a significant reduction in the size of the outer area within the neurospheres corresponding to radial glia extensions (Fig. 4A and 4B, p = <0.0001). Specifically, we found that the area covered by HOPX-expressing outer radial glia cells, which function as a glial scaffold to support neuronal migration, was substantially lower in neurospheres that underwent polyI:C stimulation (Fig. 4A and 4D, p = <0.0001).

Next, we investigated if polyI:C could influence CTIP2-expressing cells that migrate along the radial glia extensions to form the deep layers of the cortex. We found that the intensity of CTIP2 was significantly reduced within the outer area of polyI:C exposed neurospheres (Fig. 4E, p = <0.0001). Subsequently, to test whether this observation is a result of defective migration or a direct effect on the expression of CTIP2, we calculated the number of CTIP2-expressing nuclei adjusting for the size of the outer area. We found a greater number of CTIP2-expressing nuclei per mm2 in the polyI:C exposed neurospheres (Fig. 4F, p = <0.0001), suggesting that overall reduction of CTIP2 in the neurospheres is linked to halted migration due to the disorganised glial scaffold, rather than the direct effect of polyI:C on CTIP2 expression. We subsequently carried out gene expression analysis using RT-qPCR of neuronal progenitor cells. In line with our findings from our immunofluorescence experiments, we did not observe a change in CTIP2 expression following polyI:C stimulation (*supplementary figure 8*).

4. Discussion

We provide a novel neurosphere assay to model key aspects of human cortical development using iPSC derived neural progenitor cells and state-of-the-art live cell imaging and analysis. We demonstrate the ability to visualise and quantify cortical developmental processes in live human cells for the first time. This assay represents a substantial step forward in modelling human cortical development. The neurosphere assay offers several advantages over neural rosettes in cortical organoids and organotypic cultures from fetal brain tissues. First, neurospheres are highly scalable and can be made from stored neuronal progenitors providing greater experimental flexibility. Second, neurospheres offer a stage to study live individual cells and quantify developmental processes in greater detail e.g. capturing the dynamic process of radial glia extension. Third, the live cell probes do not hinder the subsequent ability to study specific makers of interest following fixation, allowing for its integration with classical immunofluorescence techniques. A key feature of our work was the accompanying automated pipeline that not only facilitated high throughput image analysis but also eliminated investigator bias linked to manual analysis techniques. Importantly, this neurosphere assay is amenable to genetic and environmental modifications, and thus offers a unique platform to study the effects of genetic and environmental risk factors linked to neurodevelopmental disorders in future research.

We applied our neurosphere assay to study the effects of a simulated viral infection. The neurospheres were constructed using neuronal progenitor cells at the start of cortical differentiation, which represents a relevant timepoint for neurodevelopmental disorders. We used polyI:C, a synthetic double stranded RNA molecule and well-established viral infection mimic, to simulate viral infection and identified that both radial glia growth and neural cell migration were substantially reduced over time. These findings were further supported by immunofluorescence experiments that demonstrated polyI:C stimulation led to reduced growth of HOPX-expressing outer radial glia scaffold, which would eventually give rise to the upper cortical layer neurons. On the other hand, the migration of CTIP2-expressing deep cortical layer cells was halted while its expression was unaffected in polyI:C exposed neurospheres. Collectively, our findings provide insight into how viral infections could lead to differential functional effects on the upper and deeper layer neurons in the developing human cortex.

The results from this study are in line with epidemiological studies that show maternal infections during pregnancy increase the risk of neurodevelopmental disorders in the offspring (Saatci et al., 2021; Jiang et al., 2016). Further, previous work by Bhat et al has shown that iPSC derived neuronal progenitors from schizophrenia patients display an attenuated transcriptional response to interferon-gamma treatment compared to controls (Bhat et al., 2022), highlighting a potential role for gene-environmental interactions. Future work using this neurosphere assay could explore this by combining gene editing techniques with infection mimics. Furthermore, previous work in rodent models support the findings from this study. In particular, maternal immune activation models have shown that polyI:C induced gene expression and methylation changes not only mapped to cortical cells but also were enriched among disease linked genes (Handunnetthi et al., 2021; Johnson et al., 2022). Furthermore, Canales *et al* found that maternal polyI:C exposure led to perturbation in neuronal migration during cortical development (Canales et al., 2021). Specifically, the authors found reductions in cortical cell populations including CTIP2- cells, which is consistent with our own observations of reduced CTIP2- cell migration in fixed neurospheres.

This study has several key strengths. The neuronal progenitors are derived from human iPSCs and thus provide insight into the unique cortical development in humans. Also, this is the first-time non-toxic live imaging probes have been used to study neural migration, providing valuable temporal insight into these dynamic processes that were not previously captured. Further, our automated analysis pipeline makes this assay high throughput and eliminates the potential for investigator bias. Although, the neurosphere assay did not directly measure cell proliferation, this can be indirectly estimated through tracking of individual nuclei and measuring neurosphere size over time in future studies. Similarly, further insight into cell differentiation can be achieved through integration of classical immunofluorescence techniques. The use of the reference Kolf_2 cell line enables replication of our findings by other laboratories. Lastly, we carried out three separate

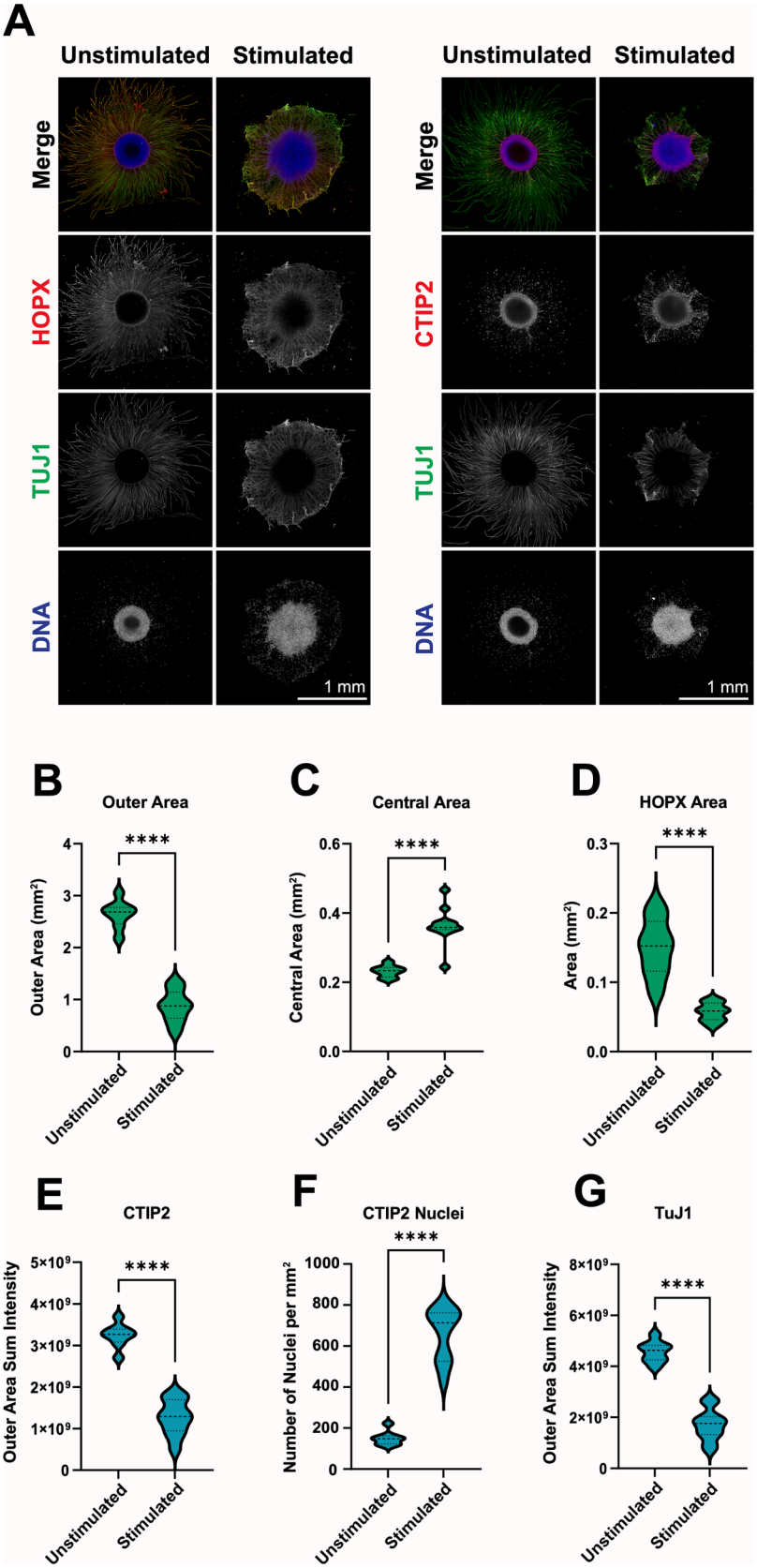

(caption on next page)

Fig. 4. The effect of viral mimic on cortical development in fixed neurospheres. A: Representative images of fixed polyI:C stimulated and unstimulated neurospheres after 48 h of growth. The expression of *HOPX*, an outer radial glia marker; and *CTIP2*, a deep layer cortical cell marker, in the stimulated and unstimulated neurospheres are shown in the left and right panels respectively. B: Comparison of outer area of neurospheres representing glial extensions between stimulated and unstimulated conditions. C: Comparison of central area of neurospheres representing unmigrated nuclei of neural cells between stimulated and unstimulated conditions. C: Comparison the HOPX area representing outer radial glia scaffold between stimulated and unstimulated conditions. E: Comparison of CTIP2 intensity in the outer area of neurospheres between stimulated and unstimulated conditions. F: Comparison of the number of CTIP2 expressing nuclei corrected for the available area of radial glia between stimulated and unstimulated conditions. G: Comparison of TuJ1 intensity presenting overall glial scaffold between stimulated and unstimulated conditions. All comparisons were carried out using unpaired and two tailed t-tests. **** = p-value < 0.0001.

neuronal differentiations that independently and reliably support our conclusions that polyI:C affects radial glia growth and neural migration.

There were also limitations to this study. First, this in vitro assay cannot fully capture the complexity of the in vivo environment made up of extracellular matrix, glial cells and vasculature that is required for successful neuronal progenitor cell migration and differentiation. Thus, further work is needed to reproduce our findings in more complex model systems. Second, polyI:C is a toll like receptor 3 agonist and cannot fully recapitulate the diverse effects of different types of viral infections as well as that of systemic effects of immune activation. However, as this neurosphere assay can easily be exposed to different immune stimuli, it is well placed to answer these questions in future studies. Along these lines, in this study the length of exposure to polyI:C was determined a priori based on established evidence on the time course of polyI:C induced gene expression (Lin et al., 2019) but further studies are needed to assess how varying exposure lengths could influence cortical developmental processes. Last, although the neurosphere assay can give some information about how early environmental exposures could exert deleterious effects on migrating cells expressing cortical layer specific markers, it cannot comprehensively study the late stages of cortical layer formation in its current from.

In conclusion, we developed a highly novel neurosphere assay to better understand key aspects of human cortical development. We combined advances in iPSC differentiation with live cell imaging techniques to shed light on the dynamic process of radial glia growth and neural cell migration. Further, this assay provides a platform to introduce genetic and environmental modifications to examine their effects on this dynamic process. To highlight this utility, we demonstrated that a viral mimic could reduce both radial glia growth and neural cell migration, providing new biological insight into how infections may exert deleterious effects on the developing human cortex.

CRediT authorship contribution statement

Edward Drydale: Methodology, Formal analysis, Investigation, Writing – review & editing. **Phalguni Rath:** Methodology, Investigation, Writing – review & editing. **Katie Holden:** Methodology, Investigation, Writing – review & editing. **Gregory Holt:** Methodology, Formal analysis, Writing – review & editing. **Laurissa Havins:** Methodology, Formal analysis, Writing – review & editing. **Thomas Johnson:** Methodology, Formal analysis, Writing – review & editing. **James Bancroft:** Conceptualization, Methodology, Resources, Writing – review & editing, Supervision. **Lahiru Handunnetthi:** Conceptualization, Methodology, Formal analysis, Resources, Writing – original draft, Writing – review & editing, Supervision, Project administration, Funding acquisition.

Declaration of competing interest

The authors declare that they have no known competing financial interests or personal relationships that could have appeared to influence the work reported in this paper.

Data availability

Data will be made available on request.

Acknowledgments

This research was supported by the National Institute for Health and Care Reseach (NIHR) Oxford Health Biomedical Research Centre United Kingdom, and John Fell Fund from the University of Oxford. The views expressed are those of the author(s) and not necessarily those of the NIHR or the Department of Health and Social Care. This work was further supported by Wellcome Trust Grants (090532/Z/09/Z and 203141/Z/16/Z) to core facilities Wellcome Centre for Human Genetics. The authors would like to thank ARIVIS for their support in developing the pipelines used for image analysis.

Appendix A. Supplementary data

Supplementary data to this article can be found online at https://doi.org/10.1016/j.bbi.2023.11.017.

References

Bhat, A., Irizar, H., Couch, A.C.M., et al., 2022. Attenuated transcriptional response to pro-inflammatory cytokines in schizophrenia hiPSC-derived neural progenitor cells. Brain Behav. Immun. 105, 82–97. https://doi.org/10.1016/j.bbi.2022.06.010.

Brennand, K., Savas, J.N., Kim, Y., et al., 2015. Phenotypic differences in hiPSC NPCs derived from patients with schizophrenia. Mol. Psychiatry 20 (3), 361–368. https://doi.org/10.1038/mp.2014.22.

Canales, C.P., Estes, M.L., Cichewicz, K., et al., 2021. Sequential perturbations to mouse corticogenesis following in utero maternal immune activation. Elife. https://doi.org/10.7554/eLife.60100.

Charlson, F.J., Ferrari, A.J., Santomauro, D.F., et al., 2018. Global epidemiology and burden of schizophrenia: findings from the global burden of disease study 2016. Schizophr. Bull. 44 (6), 1195–1203. https://doi.org/10.1093/schbul/sby058.

Delaloy, C., Liu, L., Lee, J.A., et al., 2010. MicroRNA-9 coordinates proliferation and migration of human embryonic stem cell-derived neural progenitors. Cell Stem Cell 6 (4), 323–335. https://doi.org/10.1016/j.stem.2010.02.015.

Ducker, M., Millar, V., Ebner, D., Szele, F.G., 2020. A semi-automated and scalable 3D spheroid assay to study neuroblast migration. Stem Cell Rep. 15 (3), 789–802. https://doi.org/10.1016/j.stemcr.2020.07.012.

Frances, L., Quintero, J., Fernandez, A., et al., 2022. Current state of knowledge on the prevalence of neurodevelopmental disorders in childhood according to the DSM-5: a systematic review in accordance with the PRISMA criteria. Child Adolesc. Psychiatry Ment. Health 16 (1), 27. https://doi.org/10.1186/s13034-022-00462-1.

Gulsuner, S., Walsh, T., Watts, A.C., et al., 2013. Spatial and temporal mapping of de novo mutations in schizophrenia to a fetal prefrontal cortical network. Cell 154 (3), 518–529. https://doi.org/10.1016/j.cell.2013.06.049.

Haddad, F.L., Patel, S.V., Schmid, S., 2020. Maternal Immune Activation by Poly I: C as a preclinical Model for Neurodevelopmental Disorders: A focus on Autism and Schizophrenia. Neurosci. Biobehav. Rev. 113, 546–567. https://doi.org/10.1016/j.neubiorev.2020.04.012.

Handunnetthi, L., Saatci, D., Hamley, J.C., Knight, J.C., 2021. Maternal immune activation downregulates schizophrenia genes in the foetal mouse brain. Brain Commun. 3 (4), fcab275. https://doi.org/10.1093/braincomms/fcab275.

Hansen, D.V., Lui, J.H., Parker, P.R., Kriegstein, A.R., 2010. Neurogenic radial glia in the outer subventricular zone of human neocortex. Nature 464 (7288), 554–561. https://doi.org/10.1038/nature08845.

Jiang, H.Y., Xu, L.L., Shao, L., et al., 2016. Maternal infection during pregnancy and risk of autism spectrum disorders: A systematic review and meta-analysis. Brain Behav. Immun. 58, 165–172. https://doi.org/10.1016/j.bbi.2016.06.005.

Johnson, T., Saatci, D., Handunnetthi, L., 2022. Maternal immune activation induces methylation changes in schizophrenia genes. PLoS One 17 (11), e0278155.

Lin, J.Y., Kuo, R.L., Huang, H.I., 2019. Activation of type I interferon antiviral response in human neural stem cells. Stem Cell Res. Ther. 10 (1), 387. https://doi.org/10.1186/s13287-019-1521-5.

Miller, D.J., Bhaduri, A., Sestan, N., Kriegstein, A., 2019. Shared and derived features of cellular diversity in the human cerebral cortex. Curr. Opin. Neurobiol. 56, 117–124. https://doi.org/10.1016/j.conb.2018.12.005.

Saatci, D., van Nieuwenhuizen, A., Handunnetthi, L., 2021. Maternal infection in gestation increases the risk of non-affective psychosis in offspring: a meta-analysis. J. Psychiatr. Res. 139, 125–131. https://doi.org/10.1016/j.jpsychires.2021.05.039.

Satterstrom, F.K., Kosmicki, J.A., Wang, J., et al., 2020. Large-scale exome sequencing study implicates both developmental and functional changes in the neurobiology of autism. Cell 180 (3), 568–584 e23. https://doi.org/10.1016/j.cell.2019.12.036.

Shi, Y., Kirwan, P., Livesey, F.J., 2012. Directed differentiation of human pluripotent stem cells to cerebral cortex neurons and neural networks. Nat. Protoc. 7 (10), 1836–1846. https://doi.org/10.1038/nprot.2012.116.

Vasistha, N.A., Pardo-Navarro, M., Gasthaus, J., et al., 2020. Maternal inflammation has a profound effect on cortical interneuron development in a stage and subtype-specific manner. Mol. Psychiatry 25 (10), 2313–2329. https://doi.org/10.1038/s41380-019-0539-5.

Warre-Cornish, K., Perfect, L., Nagy, R., et al., 2020. Interferon-gamma signaling in human iPSC-derived neurons recapitulates neurodevelopmental disorder phenotypes. eaay9506 Sci. Adv. 6 (34). https://doi.org/10.1126/sciadv.aay9506.

Zeidan, J., Fombonne, E., Scorah, J., et al., 2022. Global prevalence of autism: A systematic review update. Autism Res. 15 (5), 778–790. https://doi.org/10.1002/aur.2696.